Materials Today • Volume xxx, Number xx • xxxx 2020 RESEARCH

ELSEVIER

RESEARCH: Original Research

Soft rubber as a magnetoelectric material—Generating electricity from the remote action of a magnetic field

Kai Tan [1], Xin Wen [1], Qian Deng [1,*], Shengping Shen [1], Liping Liu [2], Pradeep Sharma [3,4,*]

[1] State Key Laboratory for Strength and Vibration of Mechanical Structures, School of Aerospace, Xi'an Jiaotong University, Xi'an 710049, China
[2] Department of Mechanical and Aerospace Engineering, Rutgers University, Piscataway, NJ 08854, USA
[3] Department of Mechanical Engineering, University of Houston, Houston, TX 77204, USA
[4] Department of Physics, University of Houston, Houston, TX 77204, USA

A magnetoelectric material is capable of converting a magnetic field into electricity. Wireless energy harvesting, drug delivery via remote action, multiple state memories are just some of the possible applications of this phenomenon. The magnetoelectric property is however rare and restricted either to certain hard exotic crystals that satisfy a stringent set of material symmetry constraints or painstakingly fabricated (still hard) composites. Soft materials that are capable of large deformations and are also magnetoelectric, do not exist. In this work, based on a simple mechanism predicated on a coupling facilitated by the universal electromagnetic Maxwell stress, deformability of soft matter and the embedding and stabilization of external charges, we experimentally demonstrate the transformation of silicone rubber into hitherto softest magnetoelectric material. Our material exhibits a room-temperature magnetoelectric coefficient as high as 193 mV cm^{-1} Oe^{-1} at the magnetic field of ≈ 600 Oe and the low frequency of ≈ 1 Hz. This rivals the performance of some of the best single phase and composite materials but with a capability of significant deformation.

Introduction

The magnetoelectric (ME) coupling refers to the property of a material to respond electrically when subjected to a change of external magnetic field. Materials exhibiting ME effect have several applications including magnetic sensors, data storage, drug delivery via remote action, and wireless energy harvesting [1–5]. Simultaneous existence of both magnetic and electric polarization degrees of freedom in single phase crystals is rare due to both symmetry considerations as well as the mutually contradictory nature of the quantum mechanical aspects of the atomic bonding required for their existence [6,7]. In addition, the ME coupling of single-phase materials (that do exist), such as $BiFeO_3$, Cr_2O_3, and $YMnO_3$, is very weak at room temperature [8,9]. These issues pertaining to single-phase ME materials significantly limit their applications.

To overcome the drawbacks of single-phase ME materials, composites that combine piezoelectric and magnetostrictive materials have been proposed [10–13]. Originally, $BaTiO_3$ and $CoFe_2O_4$ were used in such composites and the ME coupling coefficient was found to be slightly higher than that for single-phase ME materials [10,14]. Later, Ryu et al. significantly improved the coupling coefficient by proposing a new design for the ME composites. In the new design, a PZT ceramic disc was sandwiched between two Terfenol-D discs [15]. The ME coupling in all these composites originates from the product effect of piezoelectricity and magnetostriction, two phenomena that are commonly observed in piezoelectric and magnetostrictive materials which are invariably (mechanically) hard materials [16,17]. As shown by the middle sample marked with "ME composites"

* Corresponding authors.
E-mail addresses: Deng, Q. (tonydqian@mail.xjtu.edu.cn), Sharma, P. (psharma@uh.edu).

 https://doi.org/10.1016/j.mattod.2020.08.018

Please cite this article in press as: K. Tan et al., Materials Today (2020), https://doi.org/10.1016/j.mattod.2020.08.018

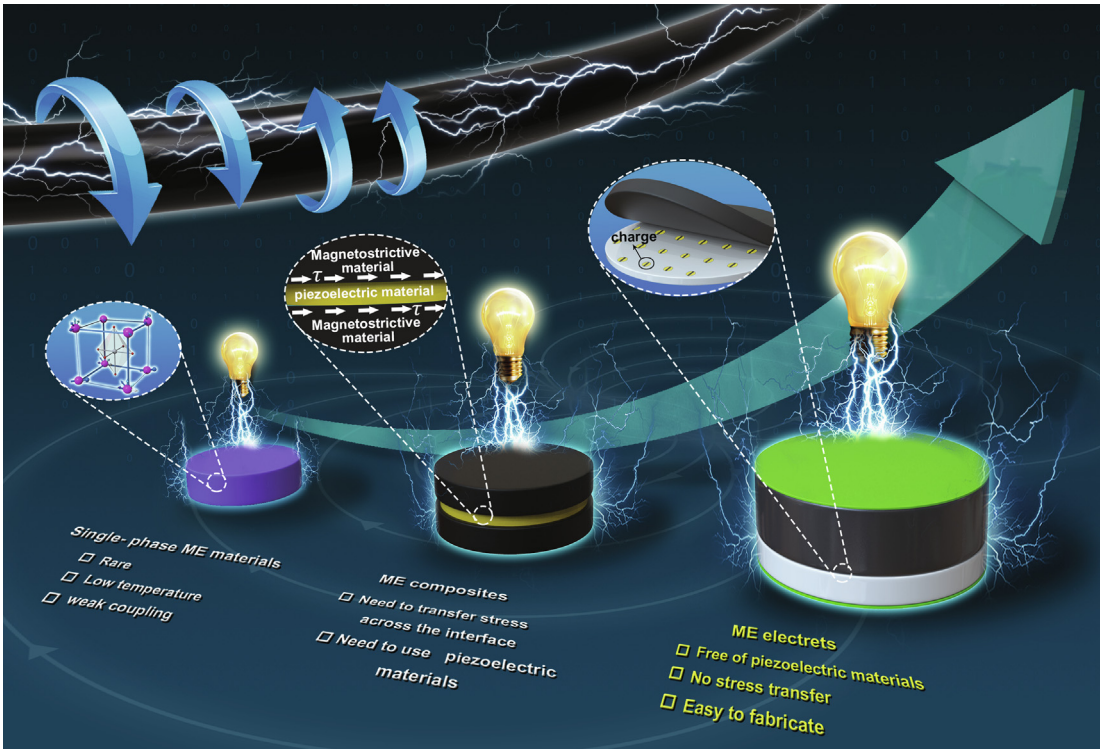

FIGUER 1

The development of ME materials: Single-phase ME materials require simultaneous existence of both magnetic and electric polarization, which is rare and exhibit only a weak ME coupling, and low operation temperature. To overcome these drawbacks, ME composites are proposed by combining magnetostrictive materials and the piezoelectric materials together. In order to ensure the high performance, an important requirement is that the magnetic field induced stress in the magnetostrictive component should be large enough and efficiently passed to the piezoelectric component. In this work, a new ME electret is proposed, in which net charges are deposited on the interface between two layers of dielectric material whose magnetic properties are different. Different from traditional ME composites, no piezoelectric material is used here, and there is no need for transferring the magnetic field induced stress between two layers.

in Fig. 1, when a magnetic field is applied across a traditional ME composite, mechanical stresses (τ) are induced in its magnetostrictive components and these stresses (marked by white arrays in Fig. 1) are transferred to the neighboring piezoelectric components which in turn generates electricity. In short, the performance of the ME composites critically depends on the properties of the piezoelectric and magnetostrictive components. In the past few decades, efforts are mostly focused on the improvement of these two components [15,18–20]. Recently, Annapureddy et al. introduced a Fe-Ga alloy for the magnetostrictive phase and obtained strong ME coupling of the composite [21]. Li et al. successfully brought a new piezoelectric member, molecular-ionic ferroelectrics, to the family of ME composites [22]. Zong et al. replaced the commonly used piezoelectric component, PZT, with cellulose [23]. In order to ensure the high performance, another requirement is that the magnetic field induced stress in the magnetostrictive component should be large enough and efficiently passed to the piezoelectric component. Due to this requirement, magnetic active elastomers (MAE) which exhibit large strain but low stress in magnetic field are usually excluded when designing high performance ME composites [24–27]. Finally, we remark that although polymers like PVDF are piezoelectric, their electromechanical coupling is quite weak and are ill-suited in the composite world to create a substantive magnetoelectric effect. In addition, at an elastic modulus of nearly 1GPa, PVDF (and materials of its kind) are not truly soft in the sense of large deformations that elastomers are capable of. In other words, truly soft materials which exhibit a substantial magnetoelectric effect do not exist. Thus, a ME material which is biocompatible, environmentally friendly, and able to endure large strain before failure, is critical for biomedical applications.

In this work, we exploit a novel mechanism predicted theoretically by us to engineer magnetoelectricity in ultra soft silicone rubber that is highly deformable and exhibits a magnetoelectric coupling rivaling that of hard composites.

Central idea and guidance from theory

As shown by the sample on the right marked with “ME electrets“ in Fig. 1, a new mechanism is introduced to engineer ME coupling in materials without involving any intrinsic piezoelectric or magnetostrictive material, or a need for passing stresses from one component to the other. The only requirement is to deposit net charges on the interface between two layers of materials which are different in magnetic properties. As we have proposed theoretically, the key idea is based on the introduction of soft electret materials and the effect of Maxwell stress [28–30].

An electret is a dielectric material with embedded quasi-permanent electrical charges or dipoles. One of the most intensely researched application of electrets is to produce strong apparent piezoelectricity in non-piezoelectric soft materials

Please cite this article in press as: K. Tan et al., Materials Today (2020), https://doi.org/10.1016/j.mattod.2020.08.018

[31–35]. Here, we use Fig. 2(a) to illustrate the central idea of the piezoelectret. As shown in Fig. 2(a), a single layer of charges is deposited on the interface between two different dielectric materials. In the figure, different colors represent different materials. Note that the Young's modulus of these two materials should be orders of magnitude different from each other in order to obtain strong apparent piezoelectricity. Then, as shown in Fig. 2(a), upon a uniaxial compression or tension, the softer layer (upper layer) deforms much more than the stiffer one (lower layer). Due to the different deformation of these two layers, the change of polarization ensues (ΔP_1, ΔP_2), which results in a change of the system's total polarization and a voltage difference between the upper and lower electrodes. The effective piezoelectric coefficient for the electret shown by Fig. 2(a) has been theoretically studied in our previous works and is given by [32]

$$d_{33}^{\text{eff}} = -\frac{2q_0H_1H_2\epsilon_1\epsilon_2}{(\epsilon_1H_2+\epsilon_1H_2)}\left(\frac{1}{Y_1}-\frac{1}{Y_2}\right) \tag{1}$$

where q_0 is the charge density of the inserted charge layer, H_1 and H_2 respectively correspond to the thickness of the upper and lower layers, $\epsilon$and Y respectively represent the permittivity and Young's modulus of the material. The subscript "1" or "2" indicates that the parameter is for the upper or lower layer. It is seen from Eq.1 that if the Young's modulus for the two layers are the same, the effective piezoelectricity vanishes ($d_{33}^{\text{eff}} = 0$). Moreover, according to Eq.1, stronger contrast between Y_1 and Y_2 results in larger d_{33}^{eff}.

It is well known that when a material is placed in an electric or/and magnetic field, the so-called is Maxwell stress develops within the body [36,37]. For a material in a magnetic field, the magnitude of its deformation depends on material's properties, such as: magnetic permeability and Young's modulus. Thus, based on this central notion and motivated by the mechanism for piezoelectrets described in the preceding section, we propose a new design for soft ME materials--the magnetoelectric electret (MEE). As shown in Fig. 1 (marked with "ME electrets"), a layer of charge is deposited on the interface between two layers of materials whose properties are different. Then, as shown in Fig. 2(b), in an perpendicularly applied uniform magnetic field, the two layered structure deforms asymmetrically, i.e., one layer deforms more than the other one. Similar to the generation of electricity in piezoelectrets shown in Fig. 2(a), this magnetic field induced asymmetric deformation also results in voltage difference between the upper and lower surfaces of the MEE. Different from traditional ME composites using piezoelectric materials, the key for the ME coupling in MEE is no longer the transferring of magnetic field induced stress from one phase to another. The magnetic active layer deforms freely. To obtain a strong ME coupling, the strain difference between the two layers should be as large as possible.

Basically, Maxwell stress exists everywhere in the magnetic field, even in the place where the relative permeability $\mu_r$is that of vacuum i.e. 1. A material deforms in the magnetic field because of the nonuniform Maxwell stress developed in it or the jump of Maxwell stress across its boundaries. For a thin plate with $\mu_r > 1$ and thickness L_0, if it is put in a uniform magnetic field h^e, and to the leading order (for illustrative purposes), the change of thickness ΔL is given by

$$\Delta L = \frac{\mu_0(1-\mu_r)^2}{Y\mu_r^2}(h^e)^2L_0 \tag{2}$$

where μ_0 is the permeability of vacuum and Y is the Young's modulus of the material. For detailed derivation, readers may refer to the Supplementary C.1. Obviously, materials with larger μ_r and smaller Young's modulus Y will deform more in a given magnetic field. Materials with μ_r equal to 1 do not deform no matter how large the imposed magnetic field.

The magnetoelectric voltage coupling coefficient α_{ME} for a ME material in magnetic field h^e is usually defined as

$$\alpha_{\text{ME}} = \frac{\mathrm{d}E}{\mathrm{d}h^e} \tag{3}$$

where E represents the induced electric field. For the MEE sample shown in Fig. 2(b), its α_{ME} is given by

$$\begin{aligned}\alpha_{\text{ME}} &= \frac{\mathrm{d}\Delta Q}{C^{\text{eff}}(L_1+L_2)\mathrm{d}h^e} \\ &= \frac{2\mu_0A_0L_1L_2\epsilon_1\epsilon_2q_0}{(L_1+L_2)C^{\text{eff}}(L_1\epsilon_2+L_2\epsilon_1)^2}\left[\frac{(1-\mu_2)^2}{Y_2\mu_2^2}-\frac{(1-\mu_2)^2}{Y_1\mu_1^2}\right]h^e\end{aligned} \tag{4}$$

where C^{eff} denotes the effective capacitance of the MEE, ΔQ is the charges flow from one electrode to the other, A_0 is the area of the electrode, q_0 represents the interfacial charge density, $L_1$and L_2 correspond to the thickness of the MEE's two layers. Similar to Eq. 1, the subscript "1" or "2" are that the material properties are for one of the two layers of the MEE. Detailed derivation for α_{ME} can be found in Supplementary Information C2. To obtain nonzero α_{ME}, one may choose materials with different $\frac{(1-\mu_r)^2}{Y\mu_r^2}$, and larger difference of this term between two layers usually leads to higher absolute value for α_{ME}.

Results and discussion

In this work, the MEE's two layers are polytetrafluoroethylene (PTFE) thin film and iron micro-particles embedded silicon rubber (IMESR) plate. Before bonding this two layers together, a layer of surface charge was deposited onto one surface of the PTFE thin film by Corona charging technique. Here, we choose PTFE thin films for two reasons: (1) the relative permeability μ_r for PTFE is very close to 1 so that it hardly deforms in magnetic field; (2) more importantly, PTFE is a good candidate for net negative charges carrier and negative charges can stay on its surface in high density for relatively long time [38]. Then the PTFE thin film and the IMESR layer are bonded together with the charged surface sandwiched in between. Finally, both the upper and the lower surfaces of the two layered structure are coated with electrodes and then we have a MEE. Upon the application of a transverse magnetic field, the PTFE layer does not deform since its $\mu_r$is almost 1. While the IMESR layer deforms in response to the magnetic field since its μ_r may be significantly larger than 1 depending on the parameter γ_{mass}, the mass ratio of mixed iron particles to the total mass. As is addressed previously, this asymmetric deformation results in the ME coupling of the MEE.

Please cite this article in press as: K. Tan et al., Materials Today (2020), https://doi.org/10.1016/j.mattod.2020.08.018

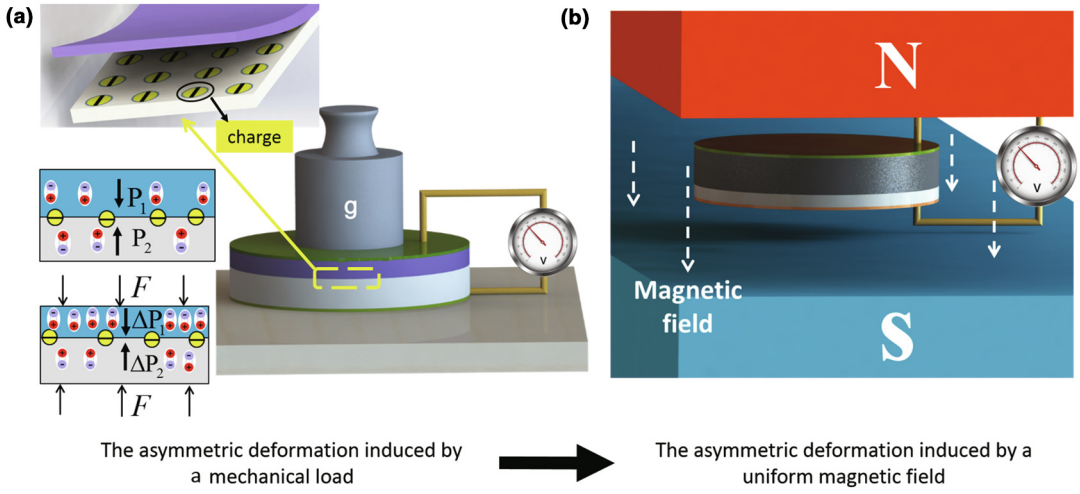

FIGURE 2

Schematic of a piezoelectret and a magnetoelectric electret (MEE). (a) The idea of piezoelectrets. Upon uniaxial compression, the upper and lower layers deform differently due to their differing Young's modulus, which results in a voltage difference across the upper and lower electrodes. (b) A MEE in uniform magnetic field. Similar to the generation of electricity in piezoelectrets, this magnetic field induced asymmetric deformation also results in voltage difference between the upper and lower surfaces of the MEE sample.

Impact of γ_{mass} on the deformability of IMESR

The IMESR layer's deformation is critical to the performance of a MEE and choosing proper value of γ_{mass} is an effective way to tune the material's deformability. Here, we choose different γ_{mass} (0, 30%, 50%, and 70%) for IMESR layers and measure their deformation in a magnetic field. Firstly, the materials' properties are measured and given in Fig. 3. It is seen from the figure that, with the increase of γ_{mass}, both Young's modulus Y, relative permeability μ_r and relative permittivity ϵ_r increase accordingly.

Then IMESR plates with the same thickness (3 mm) but different γ_{mass} are placed in a magnetic field which is uniform in space and harmonic in time. Throughout the whole work, the frequency of the magnetic field is fixed to 1 Hz and its amplitude is 627Oe. The deformations for IMESR plates with different γ_{mass} are plot in Fig. 4. As we can see from the figure, the deformation is largest for $\gamma_{\mathrm{mass}} = 50\%$. This can be explained by Fig. 3. Although increasing μ_r is helpful for developing Maxwell stress, larger Y is negative for materials to deform. Thus, there is certain intermediate γ_{mass} that is optimal for generating largest strain in IMESR layer. It is also interesting to see from Fig. 4 that the value of deformation is always positive no matter which direction the magnetic field is pointing at (upward or downward). This is because that the Maxwell stress depends on magnetic field quadratically. So reversing the direction of a magnetic field would not result in the change of Maxwell stress. For this reason, the deformation ΔL shown in Fig. 4 varies in a frequency twice of that for the magnetic field (2 Hz).

Measuring the ME coupling coefficient of the MEE

To test the performance of the proposed design of MEE, we fabricated a MEE which is composed of a PTFE thin film and a $\gamma_{\mathrm{mass}} = 50\%$ IMESR layer and placed it in the magnetic field to measure the charge flow between its upper and lower surfaces. The IMESR layer is 3 mm in thickness and the interfacial charge

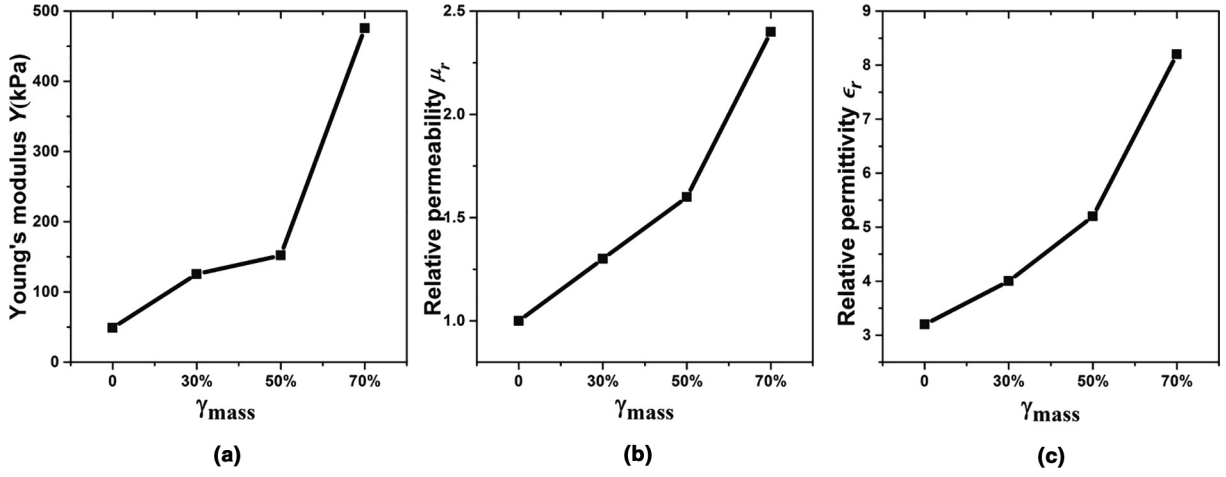

FIGURE 3

Material properties for IMESR with different γ_{mass}. (a) Young's modulus Y; (b) Relative permeability μ_r; (c) Relative permittivity ϵ_r.

Please cite this article in press as: K. Tan et al., Materials Today (2020), https://doi.org/10.1016/j.mattod.2020.08.018

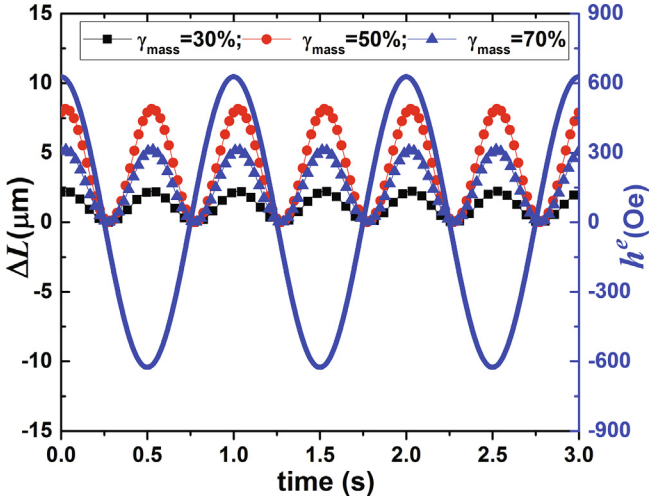

FIGURE 4

Deformation of IMESR plates with different γ_{mass} in a time variant uniform magnetic field. The blue solid line shows the variation of the magnetic field with time. Lines with marks present the deformation of different IMESR plates.

density is -1.3195mC/m^2. As shown in Fig. 5(a), the output charge ΔQ, or charges flowing between two electrodes, varies with time at a frequency of 2 Hz, twice of that for the applied magnetic field. Recall that the deformation shown in Fig. 4 also varies at a frequency of 2 Hz. This confirms the point that the ME coupling and the IMESR layer's deformation is caused by the Maxwell stress instead of the gradient of magnetic field. Fig. 5(a) also shows that without interfacial charges, the output charge drops to nearly zero, which indicates the importance of interfacial charges to the ME coupling.

In this work, with measured effective capacitance C^{eff}, α_{ME} can be written in terms of the output charge ΔQ as following:

$$\alpha_{ME} = \frac{d\Delta Q}{C^{eff} L dh^e} \tag{5}$$

where L denotes the total thickness of the MEE. The parameter C^{eff} can be measured directly using an impedance analyzer (Keysight E4990A, America). For the test sample, its C^{eff} is measured to be 16.3pF. From the plot in Fig. 5(a), one may plot the output charge ΔQ as a function of the magnetic field h^e as shown by the red line in Fig. 5(b). Based on this plot, the term $d\Delta Q/dh^e$ can be calculated numerically. The black line in Fig. 5(b) indicates the ME coupling α_{ME} as a function of the magnetic field. From the figure, it's seen that α_{ME} varies linearly with h^e. It is zero when $h^e = 0$ and reaches $193\text{mVcm}^{-1}\text{Oe}^{-1}$ when $h^e = 600\text{Oe}$. Note that, from Eq. S26 in supporting information, ΔQ is proportional to the square of h^e. Thus, the ME coupling coefficient α_{ME} linearly depends on the level of external magnetic field h^e. Actually, the dependency of α_{ME} on biased magnetic field is widely observed in existing ME composites of piezoelectric and magnetostrictive materials. Ryu et al. found that α_{ME} kept increasing from 0 to $4680\text{mVcm}^{-1}\text{Oe}^{-1}$ as h^e increased from 0 to 4200Oe[15].

It is also worthwhile to mention that the ME coupling coefficients measured in most previous works are for a specific frequency of the alternating part of the external magnetic field. At such specific frequency, the test samples usually reach their resonance and exhibit the strongest ME coupling effect. For example, $\alpha_{ME} = 4680\text{mVcm}^{-1}\text{Oe}^{-1}$ was measured in Ryu's work at the frequency of 1 kHz [15]; Zong et al. obtained$\alpha_{ME} = 1410\text{mVcm}^{-1}\text{Oe}^{-1}$ at an optimum frequency of 56.1 kHz [23]; Li et al. introduced molecular-ionic ferroelectrics to ME composites and found that α_{ME} reaches about $186\text{mVcm}^{-1}\text{Oe}^{-1}$ at the frequency of 39 kHz [22]; Annapureddy et al. reported an extremely high coefficient of $1330\text{Vcm}^{-1}\text{Oe}^{-1}$when they attached the ME composite to a cantilever beam vibrating at its resonant frequency around 100 Hz [21]. In most of the above works, it's also found that α_{ME} reduced by several tens or hundreds times if the exciting frequency was slightly shifted from the resonant frequency. In this work, our objective is to introduce a new mechanism of ME coupling rather than designing optimum structures to take the most advantage

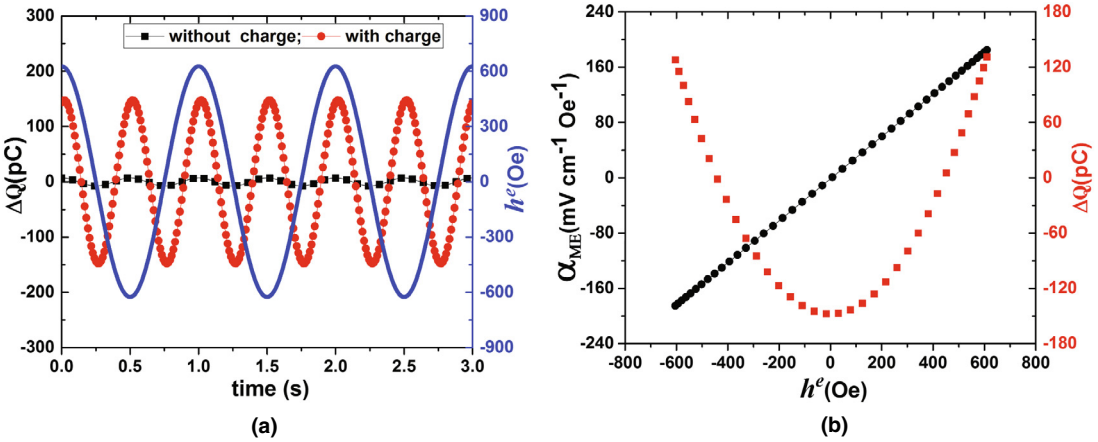

FIGURE 5

Performance of a MEE in magnetic field. (a) Variation of output charge with time. The blue solid line shows the variation of the magnetic field with time. The red line with marks represents the output charge of the MEE. The black line with marks represents the output charge for a MEE without the interfacial charges. (b) Plot of output charge and ME coupling coefficient α_{ME} as functions of magnetic field h^e.

Please cite this article in press as: K. Tan et al., Materials Today (2020), https://doi.org/10.1016/j.mattod.2020.08.018

of structure resonance. Thus, although the resonant frequency of the test sample is around 1.56 kHz, we just measured α_{ME} at 1 Hz. We believe that the value 193mVcm^{-1}Oe^{-1} we measured here is much higher than most of the reported woks if the structure resonance was not taken into account.

The effect of interfacial charge density

To further investigate the effect of interfacial charges, in Fig. 6, samples with different interfacial charge density are tested separately. The performance, both the output charge and α_{ME}, of the MEE is magnetic field dependent. In the applied time-dependent magnetic field, they vary as a sine or cosine function of time. Here, we recorded the amplitude of them (α_{ME}^{A} and ΔQ^{A}) for comparison. As shown in Fig. 6, both α_{ME}^{A} and ΔQ^{A} are proportional to the inserted interfacial charge density q_0. This conclusion agrees well with Eq.4, where α_{ME} is proportional to q_0. This conclusion also indicates that, to obtain better performance of the MEE, a good way is to increase the interfacial charge density. However, not many materials are good charges carrier. In reality, it is usually difficult to deposit very high density of charges onto the surface of a material. Here, we choose PTFE for its ability to hold negative charges strongly.

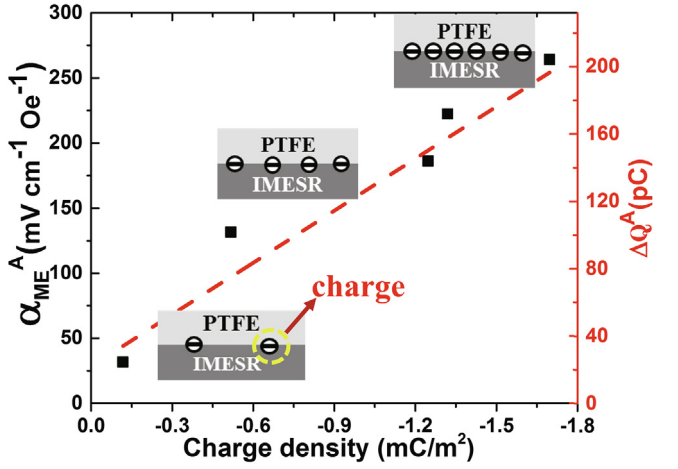

FIGURE 6

The amplitudes of α_{ME} and output charge of the MEE as functions of the interfacial charge density.

The effect of iron particles mass ratio

Now we study the impact of another key factor, the iron particles mass ratio γ_{mass}, on the performance of a MEE. Three values, 30%, 50% and 70%, are chosen for γ_{mass}. Fig. 7(a) shows the variation of α_{ME}^{A} with respect to γ_{mass} for given magnetic field and interfacial charge density ($q_0 = -1.3195\text{mC/m}^2$). It is found from the figure that $\gamma_{mass} = 50\%$ corresponds to the case of highest α_{ME}^{A}. This agrees with the observation in Fig. 4 where $\gamma_{mass} = 50\%$ corresponds to the largest deformation. It also confirms the importance of the IMESR layer's deformation to the performance of the MEE.

Fig. 7(b) shows the variation of ΔQ^{A} with respect to γ_{mass}. Different from the observation in Fig. 7(a), as γ_{mass} increases from 30% through 70%, the output charge keeps increasing instead of peaking at 50%. This is due to the fact that the effective capacitance C^{eff} of the MEE increases fast with γ_{mass}. The capacitances for samples of γ_{mass} = 30%; 50%; 70% are 13.77pF; 16.30pF; and 26.15pF, respectively. For this reason, although the voltage generated by $\gamma_{mass} = 70\%$ sample is lower than that for $\gamma_{mass} = 50\%$, the output charge for the former is larger.

The effect of IMESR layer's thickness

In addition, the impact of the IMESR layer's thickness on the MEE's performance is also studied. In this study, we fixed γ_{mass} to 50% and the interfacial charge density to $q_0 = -1.3195\text{mC/m}^2$. Three different thickness $L_I = 1$ mm, 3 mm and 5 mm are considered.

The plots in Fig. 8(a) and (b) show that both α_{ME}^{A} and ΔQ^{A} increase with the decrease of L_I. This is because that the PTFE layer is much thinner (30 μm) than the IMESR layer.

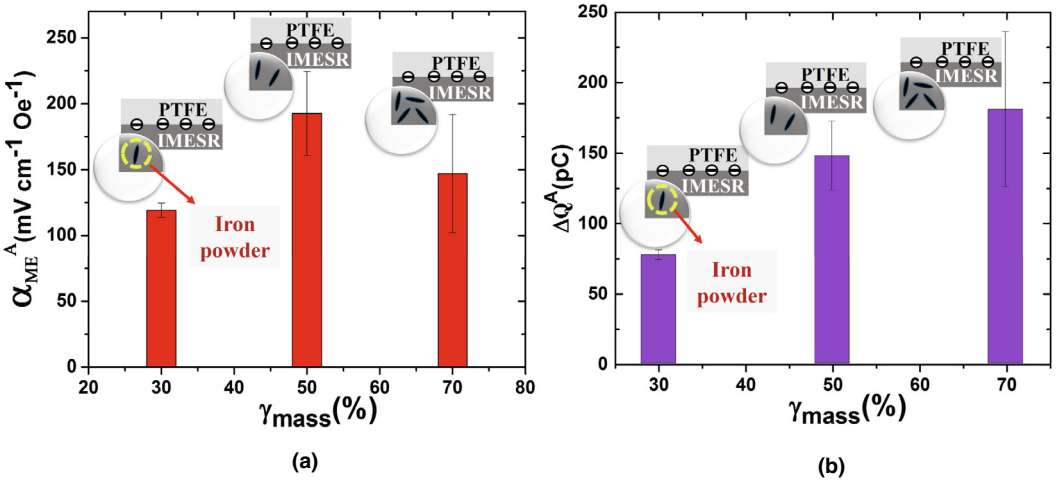

FIGURE 7

The impact of γ_{mass} on the performance of the MEE. (a) The ME coupling coefficient α_{ME}^{A} for different γ_{mass}. (b) The generation of output charges ΔQ^{A} increase with the increase of γ_{mass}.

Please cite this article in press as: K. Tan et al., Materials Today (2020), https://doi.org/10.1016/j.mattod.2020.08.018

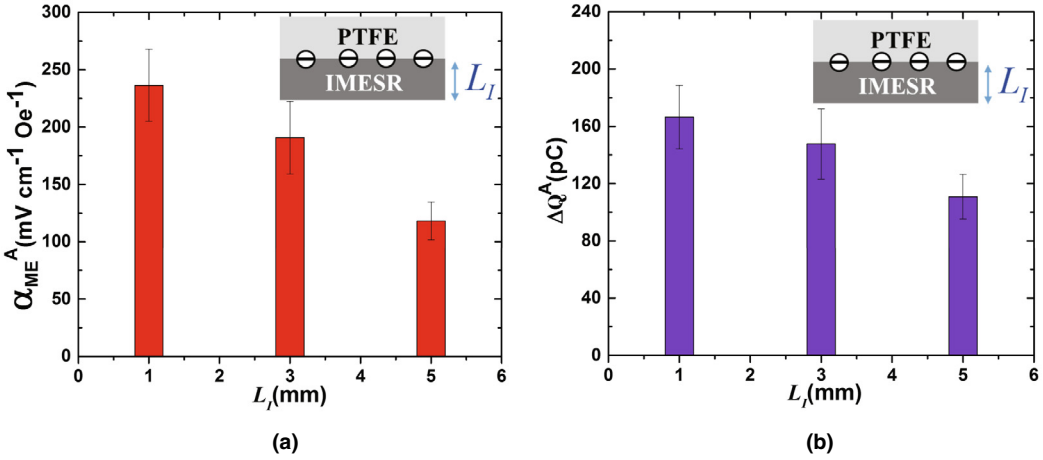

FIGURE 8

The impact of IMESR layer's thickness $L_I$on the performance of the MEE. (a) The ME coupling coefficient α_{ME}^{A} for different L_I. (b) The amplitude of output charges for different L_I.

Theoretically, to optimize the performance of the MEE, the IMESR layer's thickness should be as close to 1.3 times that of PTFE as possible (for details, one may refer to the Supplementary Information C.3). Although making the PTFE layer thicker is another way to enhance the system's performance, in reality, increasing the PTFE film's thickness is harmful to its charge storage capability. So the better way may be using thinner IMESR layers.

Piezoelectric behavior of the MEE

It's worthwhile to mention that the MEE introduced here is not only capable of converting between magnetic field energy and electricity, but also exhibits effective piezoelectricity. As is explained by Eq. 1, the difference in Young's modulus of the two layers usually results in nonzero effective piezoelectricity d_{33}^{eff}. The reported Young's modulus for PTFE is more than 500 MPa which is several thousands times higher than that for the magnetic active layer. For this reason, the MEE's d_{33}^{eff} could be not only nonzero, but also large in value.

Here, we choose $L = 3.03\text{mm}$, $q_0 = -1.3195\text{mC/m}^2$ and $\gamma_{\text{mass}} = 50\%$ for the MEE. Under a cyclic mechanical loading shown by the blue line in Fig. 9, there are charges flowing between the MEE's upper and lower surface electrodes. Different from the ME coupling behavior, the red line in Fig. 9 shows that the output charge varies with the mechanical loading synchronously. This is because that the deformation of the active layer is roughly proportional to the applied mechanical loading for the case studied here. The effective piezoelectricity d_{33}^{eff} is invariant of the applied load and was calculated to be around 47.8 pC/N.

In summary, without using any intrinsic piezoelectric materials, we synthesized a soft smart material, MEE, which shows not only ME coupling property but also effective piezoelectricity. The basic idea originates from the design of piezoelectret (or ferroelectret), a well known electret material shows effective piezoelectricity. Our research focuses on a two layered structure with net charges deposited on the interface. Different from previously reported ME composites, in the MEE introduced here, none of

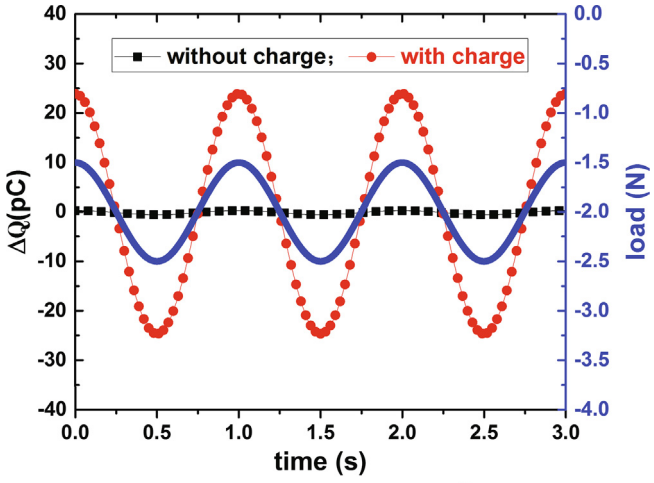

FIGURE 9

Effective piezoelectricity d_{33}^{eff} of the MEE.

the two phases is piezoelectric and there is no need for transferring stress or strain between them. Experimental results indicate that the iron particles' mass ratio (γ_{mass}), the interfacial charge density (q_0), and the thickness of the two layers of the MEE are three factors that affect its performance significantly. This work provides a new thought of designing ME composites. It is the first step to a new field of rubbery ME composites.

Methods

Measurement of material properties: The Young's modulus (Y) was obtained through uniaxial tensile tests using universal testing machine (Electroforce 3230, TA). The relative permittivity (ϵ_r) was indirectly obtained by measuring the capacitance C of the sample, and then using the following equation:

$$\epsilon_r = \frac{Cd}{\epsilon_0 A},$$

where d and A respectively denote the thickness and the surface erea of the sample. In this work, the capacitance C was measured

Please cite this article in press as: K. Tan et al., Materials Today (2020), https://doi.org/10.1016/j.mattod.2020.08.018

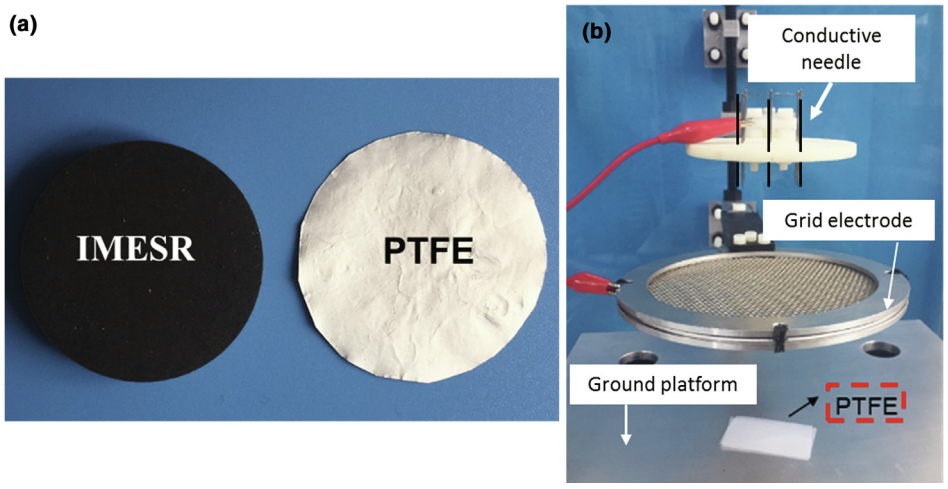

FIGURE 10

(a) An IMESR plate (left) with thickness of 3 mm and γ_{mass} = 50% and a polytetrafluoroethylene (PTFE) thin film (right) with thickness of 30 μm. (b) Corona charging setup for a PTFE thin film.

by an impedance analyzer (Keysight E4990A, America). The relative permeability (μ_r) was obtained in the following way. Firstly, the magnetic hysteresis loop was plot by Vibrating Sample Magnetometer (MPMS-squid VSM-094). Then, the initial slop of the magnetic hysteresis loop was calculated as μ_r.

Fabrication of MEE: IMESRs were prepared by mixing iron micro-particles (size less than 0.5 μm) with silicone elastomer (Ecoflex 00–10) at prescribed weight fraction. The mixture was poured into a mold to obtain desired geometry and then cured at 80 °C for 10 min. Corona charging is used to deposit charges onto the surface of a PTFE thin film metalized on another side as present in Fig. 10(a). As shown in Fig. 10(b), the conductive needle is subjected to very high DC voltage (−8 kV) and placed above a grid with much lower DC voltage (−3 kV). Under the grid, a PTFE thin film is placed on a grounded platform. The high voltage difference between the needle and the grid ionize the air molecules around the needle and accelerate the charges towards the PTFE thin film. Finally, the PTFE thin film and the IMESR layer are bonded together.

Directly measuring the surface charge density on a PTFE thin film is not trivial. Usually, an indirect way of measuring the potential (V_s) of the cressponding surface is used. Then the surface charge density (q_0) can be predicted according to the following equation [39]:

$$q_0 = \frac{\epsilon_p \epsilon_0 V_s}{L_p},$$

where ϵ_p and L_p respectively represent the permittivity and the thickness of the PTFE. In this work, the surface potential (V_s) is measured by the electrostatic voltmeter (TRek MODEL P0865).

Measurement of the magnetic field induced output charge: The performance of the MEE was investigated by

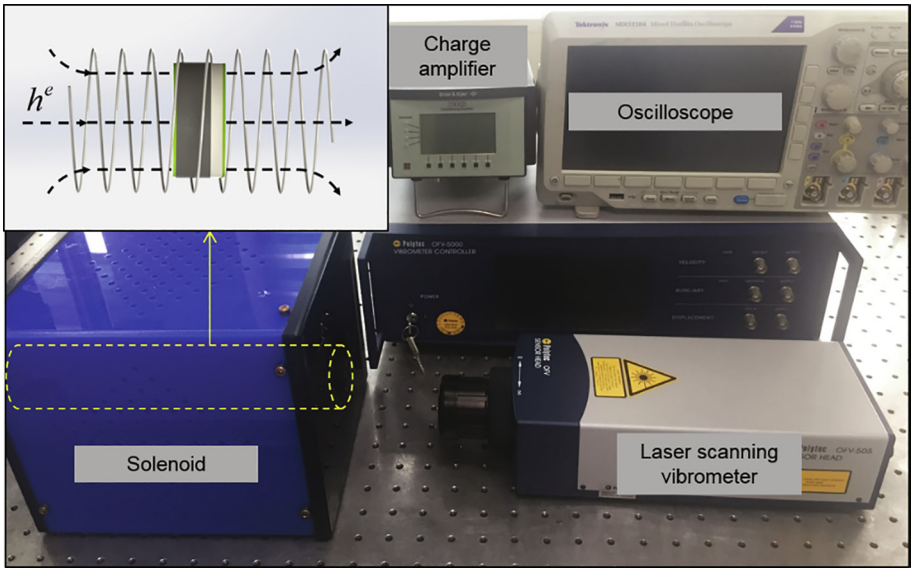

FIGURE 11

Measurement setup.

Please cite this article in press as: K. Tan et al., Materials Today (2020), https://doi.org/10.1016/j.mattod.2020.08.018

using a customized solenoid that generate AC magnetic field (h^e), as shown in Fig. 11. The deformation of this material was investigated by using Laser Scanning Vibrometer (Polytec OFV-5000, Germany). The output charge of the MEE was measured by charge amplifier (Bruel & Kjaer, Denmark) and oscilloscope (Tektronix MDO3014, America) under an external magnetic field.

Data availability

The data that support the findings of this study are available from the corresponding author on reasonable request.

Declaration of Competing Interest

The authors declare that they have no known competing financial interests or personal relationships that could have appeared to influence the work reported in this paper.

Acknowledgements

The authors KD, XW, QD and SS gratefully acknowledge the support from the National Key R&D Program of China (2017YFE0119800), the National Natural Science Foundation of China (Grants No. 11632014, No 11672222, and No 11372238), and the B1804 project of China. We thank the Instrumental Analysis Center of Xi'an Jiaotong University for their assistance with characterization. P.S was supported by the University of Houston M.D. Anderson Professorship.

Author contributions

Q.D., P. Sharma, and L.P.L. initiated the original idea; K.T and X. W led all the device modeling, design and measurements with the supervision of Q.D and S.S P; K.T analyzed the data and prepared the manuscript with the supervision of Q.D; All authors discussed the results.

Competing interests

The authors declare no competing interests.

Appendix A. Supplementary data

Supplementary data to this article can be found online at https://doi.org/10.1016/j.mattod.2020.08.018.

References

[1] J.F. Scott, Science 315 (5814) (2007) 954–959.
[2] J.P. Velev, S.S. Jaswal, E.Y. Tsymbal, Proc. R. Soc. A 369 (1948) (2011) 3069–3097.
[3] W. Eerenstein, N.D. Mathur, J.F. Scott, Nature 442 (7104) (2006) 759–765.
[4] X.-Z. Chen et al., Adv. Mater. 29 (8) (2017) 1605458.
[5] V. Annapureddy et al., Sustainable Energy Fuels 1 (10) (2017) 2040–2052.
[6] H. Schmid, Ferroelectrics 162 (1) (1994) 317–338.
[7] Nicola A Hill. Why are there so few magnetic ferroelectrics? 2000.
[8] J. Wang et al., Science 299 (5613) (2003) 1719–1722.
[9] D.N. Astrov, Sov. Phys. JETP 13 (4) (1961) 729–733.
[10] J. Van Suchtelen, Philips Res. Rep 27 (1) (1972) 28–37.
[11] C.-W. Nan, Phys. Rev. B 50 (9) (1994) 6082–6088.
[12] R.E. Newnham, D.P. Skinner, L.E. Cross, Mater. Res. Bull. 13 (5) (1978) 525–536.
[13] C.-W. Nan et al., J. Appl. Phys. 103 (3) (2008) 031101.
[14] J. Van Den Boomgaard et al., J. Mater. Sci. 9 (10) (1974) 1705–1709.
[15] J. Ryu et al., Jpn. J. Appl. Phys. 40 (8) (2001) 4948.
[16] M.G. Kang et al., Adv. Energy Mater. 8 (16) (2018) 1703313.
[17] E. Lage et al., Nat. Mater. 11 (6) (2012) 523.
[18] R.A. Islam et al., J. Appl. Phys. 104 (10) (2008) 104111.
[19] Y. Yan, Y. Zhou, S. Priya, Appl. Phys. Lett. 102 (5) (2013) 052907.
[20] J. Ma et al., Adv. Mater. 23 (9) (2011) 1062–1087.
[21] V. Annapureddy et al., Energy Environ. Sci. 11 (4) (2018) 818–829.
[22] D. Li et al., Adv. Mater. 30 (52) (2018) 1803716.
[23] Y. Zong et al., Nat Commun 8 (1) (2017) 38.
[24] S. Bednarek, Appl. Phys. A 68 (1) (1999) 63–67.
[25] J.M. Ginder et al., Int. J. Modern Phys. B 16 (2002) 472–478.
[26] X. Guan, X. Dong, J. Ou, J. Magn. Magn. Mater. 320 (3-4) (2008) 158–163.
[27] D.Y. Borin, S. Odenbach, G.V. Stepanov, J. Magn. Magn. Mater. 470 (2019) 85–88.
[28] Z. Alameh et al., J. Mater. Res. 30 (2014) 93–100.
[29] Z. Alameh et al., Soft Matter 14 (28) (2018) 5856–5868.
[30] S. Krichen, L. Liu, P. Sharma, Phys. Rev. E 96 (4) (2017) 042404.
[31] S. Bauer, R. Gerhard-Multhaupt, G.M. Sessler, Phys. Today 57 (2) (2004) 37–43.
[32] Q. Deng, L. Liu, P. Sharma, Phys. Rev. E 90 (1) (2014) 012603.
[33] Y. Zhang et al., Nano Energy 57 (2019) 118–140.
[34] J. Zhong et al., Nano Energy 37 (2017) 268–274.
[35] X. Zhang, L. Wu, G.M. Sessler. Energy scavenging from vibration with two-layer laminated fluoroethylenepropylene piezoelectret films. In 2015 Joint IEEE International Symposium on the Applications of Ferroelectric (ISAF), International Symposium on Integrated Functionalities (ISIF), and Piezoelectric Force Microscopy Workshop (PFM), pages 24-27. IEEE, 2015.
[36] L. Liu, P. Sharma, Phys. Rev. E 88 (4) (2013) 040601.
[37] L. Liu, J. Mech. Phys. Solids 63 (2014) 451–480.
[38] S. Gong et al., Adv. Funct. Mater. (2019) 1807618.
[39] R. Collins, Appl. Phys. Lett. 26 (12) (1975) 675–677.

Please cite this article in press as: K. Tan et al., Materials Today (2020), https://doi.org/10.1016/j.mattod.2020.08.018